

# Appropriate Dose of Dapagliflozin Improves Cardiac Outcomes by Normalizing Mitochondrial Fission and Reducing Cardiomyocyte Apoptosis After Acute Myocardial Infarction

Zhong-guo Fan<sup>1</sup>, Yang Xu<sup>1</sup>, Xi Chen<sup>1</sup>, Ming-yue Ji<sup>1,2</sup>, Gen-shan Ma<sup>1</sup>

<sup>1</sup>Department of Cardiology, Zhongda Hospital, School of Medicine, Southeast University, Nanjing, People's Republic of China; <sup>2</sup>Department of Cardiology, Lianshui People's Hospital, Huaian, People's Republic of China

Correspondence: Gen-shan Ma, Department of Cardiology, Zhongda Hospital, School of Medicine, Southeast University, Nanjing, 210009, People's Republic of China, Tel +86-13002580569, Email magenshan\_D@163.com

**Objective:** Dapagliflozin (DAPA) has been reported to have significant cardiac protective effects on heart failure (HF). However, the dose and time, as well as the underlying mechanisms, for DAPA treatment in acute myocardial infarction (AMI) remain controversial. The aim of this study aimed to assess the efficacy and safety of DAPA treatment along with an increased concentration gradient for AMI and explore the potential mechanisms.

**Methods:** Non-diabetic Sprague-Dawley rats were used for establishing AMI models and then were treated with three different concentrations of DAPA [0.5 mg/kg, 1 mg/kg and 1.5 mg/kg, described as AMI+DAPA Low, AMI+DAPA Medium (Med) and AMI+DAPA High, respectively] for six weeks from the onset of AMI. Echocardiography, histological staining and Western blot were performed to assess the relevant cardiac protective effects. Mitochondrial biogenesis and myocardial apoptosis were evaluated via the electron microscopy and TUNEL assay, respectively, as well as the Immunoblotting. In vitro, H9c2 cells were subjected to hypoxic treatment to assess the efficacy of DAPA on mitochondrial biogenesis and apoptosis.

**Results:** The medium dose of DAPA treatment could significantly reduce the infarct size ( $P < 0.01$ ) and the echocardiography results showed that the MI-induced damage in cardiac function got partly repaired, showing no significant difference in left ventricle ejection fraction (LVEF) versus the Sham group (Sham vs AMI+DAPA Med group: 70.47% vs 61.73%). The Western blotting results confirmed the relevant benefits and the underlying mechanisms might be through the activation of PGAM5/Drp1 signaling pathway to normalize the mitochondrial fission and reduce cardiomyocyte apoptosis. Moreover, a medium dose of DAPA treatment could avoid increased damage to the bladder endothelium following higher treatment doses.

**Conclusion:** Appropriate dose of DAPA treatment could improve the cardiac remodeling and reduce the cardiomyocyte apoptosis after AMI, without increased damage to bladder endothelium, which might be more preferred for MI patients without diabetes.

**Keywords:** Dapagliflozin, acute myocardial infarction, mitochondrial fission, cardiomyocyte apoptosis

## Introduction

Although the techniques of revascularization have become increasingly mature, acute myocardial infarction (AMI) and its sequelae are still the dominant causes of mortality all over the world.<sup>1,2</sup> Moreover, the onset of AMI has been the trend of younger, mainly because of their various unhealthy life habits.<sup>3</sup> Of note, the complete loss of blood flow to the myocardium leads to a large amount of cardiomyocyte death, triggering the inevitable myocardial remodeling and then heart failure (HF) and sudden cardiac death.<sup>4</sup> Once HF occurs, the therapeutic tools become limited, especially for those with type 2 diabetes mellitus (T2DM).<sup>5,6</sup> The emergency recanalization performed as soon as possible is strongly emphasized and great efforts are also prompted in researching the potential gene therapy to improve the cardiac remodeling post MI, leading to lower mortality rate and better prognosis.<sup>7-10</sup>

Dapagliflozin (DAPA), a sodium-glucose co-transporter 2 inhibition (SGLT2i), has been widely served as a new anti-diabetic agent,<sup>11</sup> which is also primarily demonstrated for better clinical outcomes in HF patients with T2DM.<sup>12</sup> The Dapagliflozin and Prevention of Adverse Outcomes in Heart Failure (DAPA-HF) trial subsequently strengthened and refreshed the advantages of this new agent, indicating that DAPA could significantly decrease the risk of worsening HF or cardiac death in HF patients with a reduced ejection fraction (HFrEF), regardless of the presence or absence of diabetes.<sup>13</sup> Similar positive results were also reported by another two large randomized clinical trials (RCT) of SGLT2i, showing that Empagliflozin was associated with a lower risk of cardiovascular death or hospitalization in the same patient subsets.<sup>14,15</sup> The clinical benefits of SGLT2i seem to be fully demonstrated in HF, but the relevant in vivo mechanisms remain controversial, especially in AMI.

In fact, there several potential mechanisms with respect to the cardioprotective effects of SGLT2i had been reported in diabetic hearts, among which a widely accepted concept was that SGLT2i could regulate the energy metabolism towards ketone utilization by modulating the mitochondrial dynamic and morphological function<sup>16,17</sup> and act as an antioxidant to prevent diabetic angiopathy.<sup>18,19</sup> On the other hand, SGLT2i also exhibited markable anti-inflammatory effects by regulating the macrophage polarization via STAT3 signaling or inhibiting the PI3K/AKT/mTOR pathway in infarcted hearts without diabetes.<sup>20,21</sup> However, either DAPA or empagliflozin administered in the aforementioned studies were not quite suitable for clinical practice in dose and time, which may limit expanding its cardioprotective effects or finding the potential side effects. Recently, Liu et al<sup>22</sup> conducted an experiment with the purpose of exploring for a suitable dose of empagliflozin for MI without diabetes and found that 10 mg/kg per day of empagliflozin could also act as a cardioprotective role by inhibiting cardiomyocyte apoptosis and improving cardiac remodeling via activating AMPK $\alpha$  signaling pathway in the early phase of MI. For similar purposes, we conducted this present study to assess the efficacy and safety of DAPA treatment along with an increased concentration gradient from the onset of AMI and explore for potential mechanisms.

## Method

### Animal Experiments

#### Ethical Approval and Experimental Animals

The experimental protocol was approved by the Animal Ethical Committee of Southeast University following the National Institutes of Health (NIH) guidelines for care and use of Laboratory Animals strictly (Ethical approval number: 20200326014). Sprague-Dawley rats (male, 4 weeks old) weighing 200–220 g were purchased from the Animal Center of Nanjing Medical University and then were housed under a pathogen-free condition at a temperature of  $20 \pm 2^\circ\text{C}$ , humidity of 50–70% and a regular 12 h light–dark cycle. As usual, these animals were fed with standard chow and water for 1 week before any operative procedures. All studies involving animals are reported according to the ARRIVE guidelines.<sup>23</sup>

#### Establishment of AMI Models and Treatments

After a 1-week acclimatization, 10% of chloral hydrate (3 mL/kg) was intraperitoneally injected for anaesthesia, and then a tracheal intubation was performed, connecting with a small animal ventilator (ALC-V8S; Shanghai Alcott Biotech Co., Ltd., Shanghai, China). We ligated the proximal left anterior descending (LAD) coronary artery using a 5–0 silk suture and lead II ECG was monitored during the entire procedure. A successful MI operation was confirmed by exhibiting a persistent ST segment elevation  $\geq 0.2$  mV and a general observation of the rapid discoloration over the anterior surface. Conversely, sham-operated rats underwent all the surgical procedures but without ligating proximal LAD coronary artery. By the end of surgery, all rats were intramuscularly injected with penicillin sodium (400,000 units) to prevent potential infections.

All AMI rats were randomly subdivided into four groups and administered either by vehicle or DAPA (AstraZeneca Co.) from the day after surgery. Accordingly, DAPA was dissolved in 10 mL of normal saline solution (1 mg/mL)<sup>20</sup> and administered daily via oral gavage in three different concentrations along gradient [0.5 mg/kg, 1 mg/kg and 1.5 mg/kg, described as AMI+DAPA Low, AMI+DAPA Medium (Med) and AMI+DAPA High, respectively], while the equal-volume saline solution alone was administered daily to the residual AMI rats as a control group (recorded as AMI

+Vehicle), as well as these sham-operated rats (described as Sham). After 6 weeks of treatment, rats were anaesthetized to collect blood samples from left ventricles (LV), and then the heart and bladder were rapidly removed for further analyses. It should be noted that a small infarction was considered if the visual infarct size was less than 15%, which would be hemodynamically fully compensated and then were excluded from the final analyses.<sup>24</sup>

### Assessment of Cardiac Function

To evaluate the cardiac function post MI, the transthoracic M-mode and two-dimensional echocardiography was performed at 3 weeks and 6 weeks after surgery, respectively, using the Vevo2100 imaging system (Fujifilm Visual Sonics, Inc., Toronto, Ontario, Canada) with a 21 MHz phased array linear transducer as previously described.<sup>18</sup> All rats were anesthetized via inhaling 3% of isoflurane initially and maintained with 1.5% of isoflurane during the examinations. The LV fractional shortening (FS) and ejection fraction (EF) were calculated relied on the formula as previously described.<sup>25</sup>

### Blood Measurements

One week before the sacrifice, the fasting blood glucose was measured directly from the tail tip with an animal glucometer (Sinocare Inc., Changsha, Hunan, China). At sacrifice, the blood samples were drawn from LV and the serum after centrifugation were used for further measurements of biomarkers.

### Histopathology and Infarct Size Measurements

Tissues, including left ventricles and bladders, were fixed in 4% formaldehyde and embedded in paraffin wax, then were cut into 4- $\mu$ m sections and stained with hematoxylin–eosin (H&E; hematoxylin solution and 1% eosin solution, at room temperature for 10 min each). Masson's trichrome staining and Collagen I immunohistochemistry were performed on heart tissues for measuring the infarct size according to the prior protocols.<sup>25</sup> All images were acquired using a light microscope (Nikon Corporation, Tokyo, Japan) under a high magnification and at least 2 fields in each tissue section were selected for further analyses. Moreover, a VS200 scanner (Olympus Corporation, Japan) was used for digitizing the stained heart tissue sections to make sure imaging 100% of each section. The infarct size of each digitized image was quantified via calculating the ratio of the area of interstitial fibrosis (the blue pixel content, excluding the perivascular fibrotic areas) to the total area of LV anterior wall (the red pixel content), using the Image Pro Plus software (Version 6.0; Media Cybernetics, Inc., Rockville, MD, USA) as previously described.<sup>26</sup>

### Electron Microscopy

The tissues near cardiac apex were fixed in 2.5% glutaraldehyde overnight (4°C) and then repeatedly fixed with 1% osmium tetroxide. After dehydration, the tissues were embedded in araldite CY 618 and cut into 50-nm slides. After staining with uranium acetate, these slides were observed for mitochondria under an electron microscope (HT7700 120kv, Hitachi, Japan) at 1500 $\times$  magnification directly. Mitochondrial contents were recorded as the areas taken from mitochondria versus those of cardiomyocytes analyzed with Image Pro Plus software (Version 6.0; Media Cybernetics, Inc., Rockville, MD, USA) following a prior study.<sup>27</sup>

### TUNEL Staining

After fixation in 4% paraformaldehyde, the infarcted LV tissues were embedded in paraffin wax and then cut into 3- $\mu$ M sections. These sections were detected for apoptosis levels using Terminal deoxynucleotidyl transferase-mediated dUTP nick-end labeling (TUNEL) staining, following the Manufacturer's instructions.

## Cell Experiments

### Cell Culture and Treatment

H9c2 cell lines derived from rat heart were purchased from Shanghai Institute of Biochemistry and Cell Biology (C11995500BT, Shanghai, China) and were cultured in a DMEM-low glucose medium with 10% fetal bovine serum (FBS) (Gibco; Thermo Fisher Scientific, Inc.). Normally, the cultural mediums were maintained in the condition with 5% CO<sub>2</sub> and 95% air at 37°C (labeled as the "Normoxia group"). To induce hypoxia, the serum-free culture mediums were placed in an anoxic box (C-31, Mitsubishi GS Chemical Engineering-Plastics Co., Ltd., Shanghai, China) containing the

anaerobic bag with a hypoxia indicator (C-04, Mitsubishi GS Chemical Engineering-Plastics Co., Ltd., Shanghai, China). The anaerobic system could reduce the 50% of O<sub>2</sub> concentration within 30 min and 3 hours later, the O<sub>2</sub> concentration would be reduced to <0.1%. To determine the optimal tolerance duration, the cell lines were incubated under hypoxic conditions for five time points along a time gradient, spanning 0 h to 48 h. The cells in either normoxia or hypoxia group needing DAPA (20 μM, HY-10450, Med Chem Express) treatment should be pretreated for half an hour and then maintained in each corresponding condition, recorded as Normoxia+DAPA and Hypoxia+DAPA, respectively.

### Small Interfering RNA Transfection

To suppress the expression of PGAM5, these cells incubated for hypoxia groups were transfected with specific small interfering RNA (siRNA, 100 nM/1.5x10<sup>5</sup> cells) when reaching 50% confluence. The used oligo sequence was as followed: 5'-CACUGUCACUCAUUAACCUTT-3'. Moreover, the parallel group was transfected with a negative control siRNA, described as "NC group". Lipofectamine RNAiMax (Invitrogen; Thermo Fisher Scientific, Inc.) was used for transfection in accordance with the manufacturer's instruction. After incubating for 72 h, the Western blotting was performed to confirm the transfection efficiency and determine the alterations in the protein expression levels of several target genes among these cells.

### Western Blot Analysis

Protein homogenates were obtained from whole cells and infarcted heart tissues using a RIPA buffer, respectively. A BCA protein assay kit (Thermo; USA) was used to confirm the protein concentrations. Hereafter, protein samples (30–60 μg) were separated on 8–12% SDS-PAGE gel as appropriate and transferred to a polyvinylidene fluoride (PVDF) membrane. After blocking in 5% skim milk for 1.5 h at 37 °C, these membranes were incubated with the following primary antibodies: GAPDH (1:10000; #ab8245, Abcam), β-Actin (1:1000; #ab8227, Abcam), dynamin-related protein 1 (DRP1) (1:1000; #ab184247, Abcam), fusion protein mitofusin 1 (Mfn1) (1:1000; #13798-1-AP, Proteintech Group Inc., Wuhan, China), fusion protein mitofusin 2 (Mfn2) (1:1000; #12186-1-AP, Proteintech Group Inc., Wuhan, China), phosphoglycerate mutase 5 (PGAM5) (1:500; #SC-515880, Santa, USA), Caspase3 (1:1000; #19677-1-AP, Proteintech Group Inc., Wuhan, China), Endoglin (1:1000; #10862-1-AP, Proteintech Group Inc., Wuhan, China) and β-myosin heavy chain (β-MHC) (1:1000; #10799-1-AP, Proteintech Group Inc., Wuhan, China). The Image J software (Version 1.52p, National Institutes of Health, USA) was used for quantifying protein band intensities.

### Statistical Analysis

All the results were recorded as mean ± SD and GraphPad Prism software (Version 5.0, San Diego, USA) was used for the whole analysis. Comparisons between multiple groups were conducted via 1-way or 2-way ANOVA with a post hoc Bonferroni corrections, as appropriate. All *p* values are two tailed, and statistical significance will be considered if the *p* value is less than 0.05.

## Results

### Experiments in vivo

A total of 40 rats underwent MI surgery and were then randomly subdivided into four groups. There 8 rats died of ventricular fibrillation or pneumothorax during the surgery procedures. As a supplement, 3 rats with small infarction were excluded from the final analysis. No mortality was observed throughout the study, and the 29 MI rats and 5 sham rats were finally analyzed, recorded as follows: a. Sham: *n* = 5; b. AMI+Vehicle: *n* = 8; c. AMI+DAPA Low: *n* = 6; d. AMI +DAPA Med: *n* = 9; e. AMI+DAPA High: *n* = 6.

### Efficacy and Safety of Dapagliflozin

As summarized in Table 1, DAPA could significantly decrease the blood glucose when compared to vehicle-treated groups, and its hypoglycemic effect would not get enhanced again although higher doses were applied when reaching the effective concentration. Serum creatinine showed no difference between these groups, as well as the serum K<sup>+</sup>, Na<sup>+</sup> and

**Table 1** Weight, Serum Parameters in Each Group

Parameter	Sham	AMI+Vehicle	AMI+DAPA Low	AMI+DAPA Med	AMI+DAPA High
Weight, g	377.50±31.51	391.08±28.87	346.83±27.94	372.99±37.67	357.75±16.68
Cr, mmol/L	51.76±18.60	37.81±13.31	43.10±6.37	42.10±11.94	44.10±10.06
BUN, mg/dl	19.37±2.92	19.46±1.62	28.89±1.94* <sup>#</sup>	24.68±3.58* <sup>#</sup>	28.99±3.40* <sup>#</sup>
Glu, mmol/L	9.44±2.15	11.71±2.38	4.90±0.83* <sup>#</sup>	5.64±1.32* <sup>#</sup>	5.17±0.72* <sup>#</sup>
K <sup>+</sup> , mmol/L	4.19±0.16	3.98±0.15	4.08±0.61	4.18±0.38	4.19±0.48
Na <sup>+</sup> , mmol/L	138.13±9.78	143.34±7.12	133.23±6.39	141.82±9.08	138.65±4.40
Ca <sup>2+</sup> , mmol/L	2.50±0.04	2.35±0.08*	2.49±0.02 <sup>#</sup>	2.45±0.08 <sup>#</sup>	2.52±0.02 <sup>#</sup>
P, mmol/L	2.73±0.30	2.30±0.12	2.75±0.39	2.46±0.36	2.60±0.24

Notes: \*P < 0.05 vs Sham; <sup>#</sup>P < 0.05 vs AMI + Vehicle; n=5-9 for each group.

Abbreviations: AMI, acute myocardial infarction; BUN, blood urea nitrogen; Cr, creatinine; DAPA, dapagliflozin; Glu, glucose; Med, medium; P, phosphorus.

phosphorus (P). Instead, the decrease in serum Ca<sup>2+</sup> in AMI+Vehicle group were eliminated after receiving DAPA treatment. These results indicated the positive systematic effects and relative safety of DAPA treatment.

### Dapagliflozin Attenuated Cardiac Fibrosis and Improved Cardiac Function

The MI models were established by ligating the proximal LAD artery. After six weeks, the hearts in each group were harvested for histopathology staining analyses. As depicted in [Figure 1A](#), obvious healing scars were distinguished in the anterior wall of left ventricle (LV) and DAPA favorably prevented the great damage to myocardial fibers and reduced the accumulation of collagen fibers, leading to smaller infarct size ([Figure 1B](#)). Besides, the benefits got gradually enhanced when higher doses were applied, suggesting that DAPA exerted anti-fibrotic effects. Simultaneously, markable damage to bladder endothelium was observed in DAPA treated groups, which would also get enhanced along the increased doses ([Figure 1C](#)).

Based on the echocardiography results, markable ventricular dilatation and thinning was observed after MI, reflected by a 19% increase in LVID and a ~25% reduction in thickness of interventricular septum (IVS), resulting in a significant decrease of LVEF and FS ([Figure 2A and B](#), [Supplementary Table 1](#)). As expected, DAPA could partly repair the MI-induced damage in cardiac function, showing no significant difference in EF versus the Sham group. Instead, only the medium dose of DAPA was associated with relatively improved FS and more importantly, the results at 6 weeks showed a trend of increase in EF and FS in DAPA med group compared to that at 3 weeks, suggesting that the specific dose of DAPA treatment might work better. Additionally, the protein expression level of  $\beta$ -MHC increased significantly when low and medium doses of DAPA were administered, indicating a much better LV systolic function ([Figure 2C](#)). Conversely, an interesting finding showed a significant reduction of  $\beta$ -MHC expression in the high-dose group, which might tip a potential side effect regarding the higher dose. Kapur et al<sup>28</sup> had demonstrated that decreased expression of Endoglin could reduce cardiac fibrosis and improve the survival of HF. As shown in [Figure 2D](#), there were no significant difference in Endoglin expression levels between these groups but a trend toward reduction was associated with the medium dose of DAPA. Consequently, DAPA would partly alleviate the remodeling and lead to better cardiac functions after MI, and appropriate doses might work better.

### Effects of Dapagliflozin on Mitochondrial Biogenesis

Under the electron microscopy, mitochondrial morphology and structure within the infarcted myocardium were severely broken in vehicle-treated group, taking the form of vacuolar degeneration and disappearance of the endoplasmic reticulum ([Figure 3A](#)). In DAPA-treated groups, especially in the DAPA Med group, the morphology and structure of mitochondria showed a trend of normalization. Besides, higher mitochondrial area ratio and mitochondrial counts were both observed in AMI+DAPA Med group compared to the AMI+Vehicle group ([Figure 3B and C](#)). It had been demonstrated that Drp1 could physically segregate dysfunctional mitochondrial components into a depolarized daughter organelle targeted for mitophagy to control the mitochondrial quality.<sup>29</sup> Accordingly, the Immunoblotting results indicated a significant decrease of Drp1 in the AMI+Vehicle group, which could be markedly upregulated after treating with the medium dose of DAPA ([Figure 4A](#)). The protein expression levels of mfn1/mfn2 showed no significance

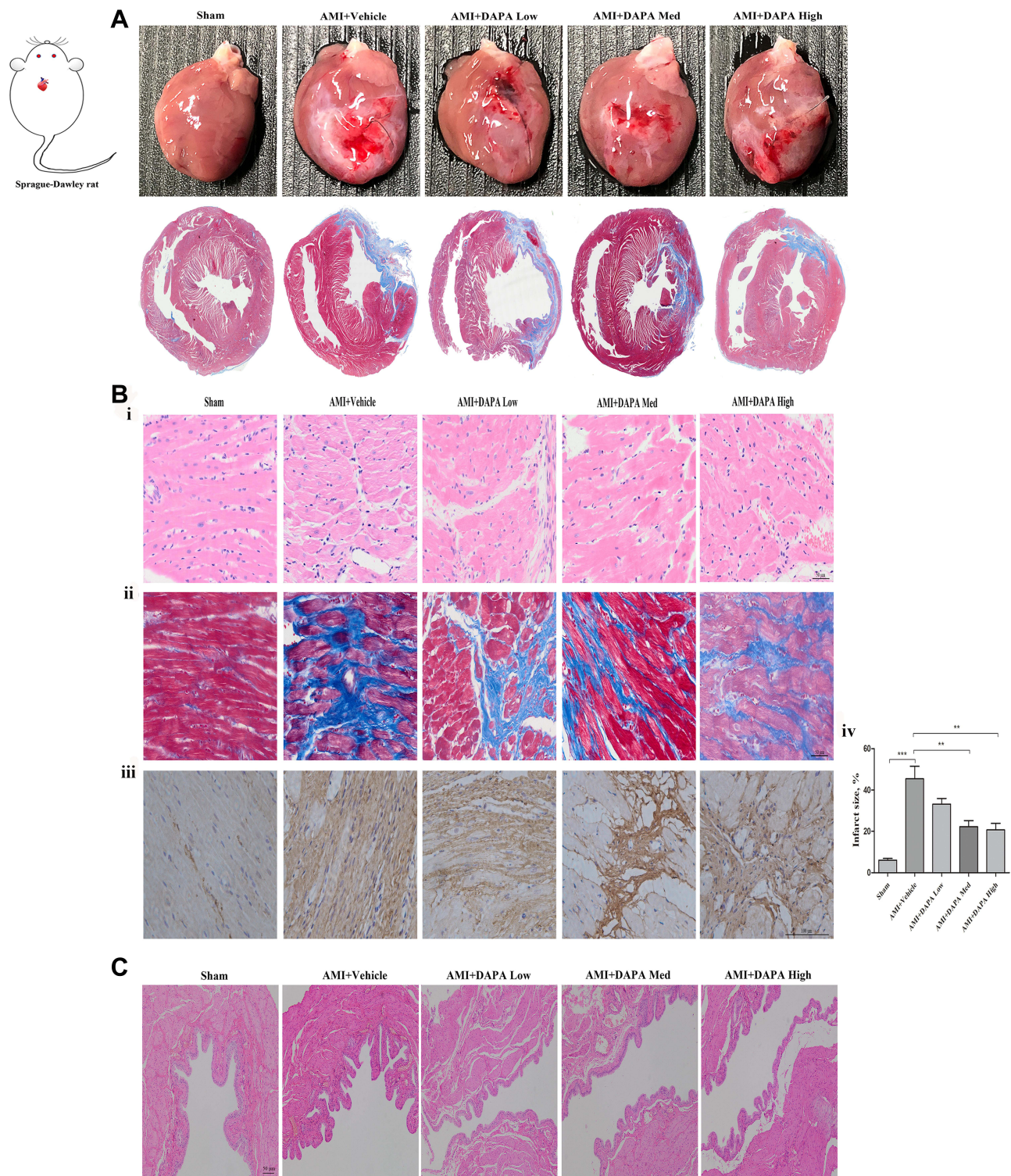


**Figure 1** Dapagliflozin attenuated cardiac fibrosis post MI, but induced markable damages to the bladder endothelium along an increased treatment dose. **(A)** The overall heart size from visual assessment and Masson staining for sham, AMI+Vehicle, AMI+DAPA Low, AMI+DAPA Med and AMI+DAPA High group, respectively. **(B)** Histopathological observations of rat heart tissues: i) HE staining, ii) Masson staining, iii) collagen I immunohistochemistry and iv) calculation of infarct size in each group. **(C)** H&E staining of bladder tissues from each group.  $N \geq 3$  per; Data are mean $\pm$ SD.  $**P < 0.01$ ,  $***P < 0.001$ . AMI: acute myocardial infarction, DAPA: Dapagliflozin, Med: medium.

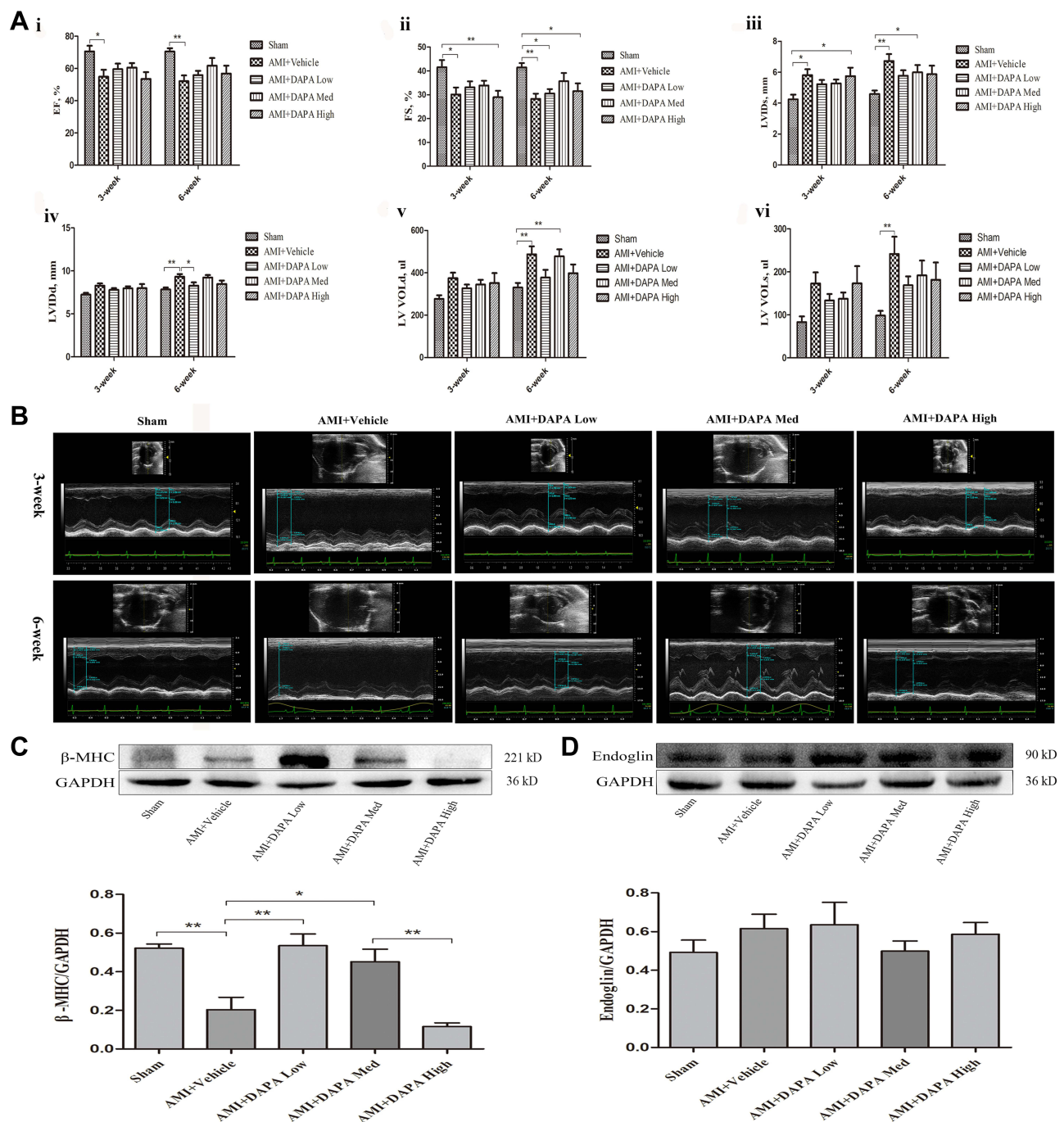


**Figure 2** Dapagliflozin improved cardiac function in MI rats. **(A)** Alterations in cardiac structure and function based on echocardiography: i) the ejection fraction (EF); ii) the fractional shortening (FS); iii) the left ventricular systolic internal dimension (LVIDs); iv) the left ventricular diastolic internal dimension (LVIDd); v) the left ventricular volume in systole (LV VOLS) and vi) the left ventricular volume in diastole (LV VOLD) among Sham, AMI+Vehicle, AMI+DAPA Low, AMI+DAPA Med and AMI+DAPA High group, respectively. **(B)** Doppler echocardiographic images obtained from hearts of rats from different groups. **(C)** Representative Western blots and quantitative analyses for  $\beta$ -myosin heavy chain ( $\beta$ -MHC) and **(D)** Endoglin protein expression levels normalized to GAPDH.  $N \geq 3$  per; Data are mean $\pm$ SD. \* $P < 0.05$ , \*\* $P < 0.01$ .

between these groups (Figure 4B and C). Taken together, these results suggested that DAPA could normalize the mitochondrial fission linked to mitochondrial dynamism within the infarcted myocardium.

### Dapagliflozin Reduced Cardiomyocyte Apoptosis

PGAM5 is a mitochondrial membrane protein which can interact with Drp1 to play as a crucial role in response to necroptosis and apoptosis.<sup>30,31</sup> We investigated the protein expression level of PGAM5 and found that a medium dose of

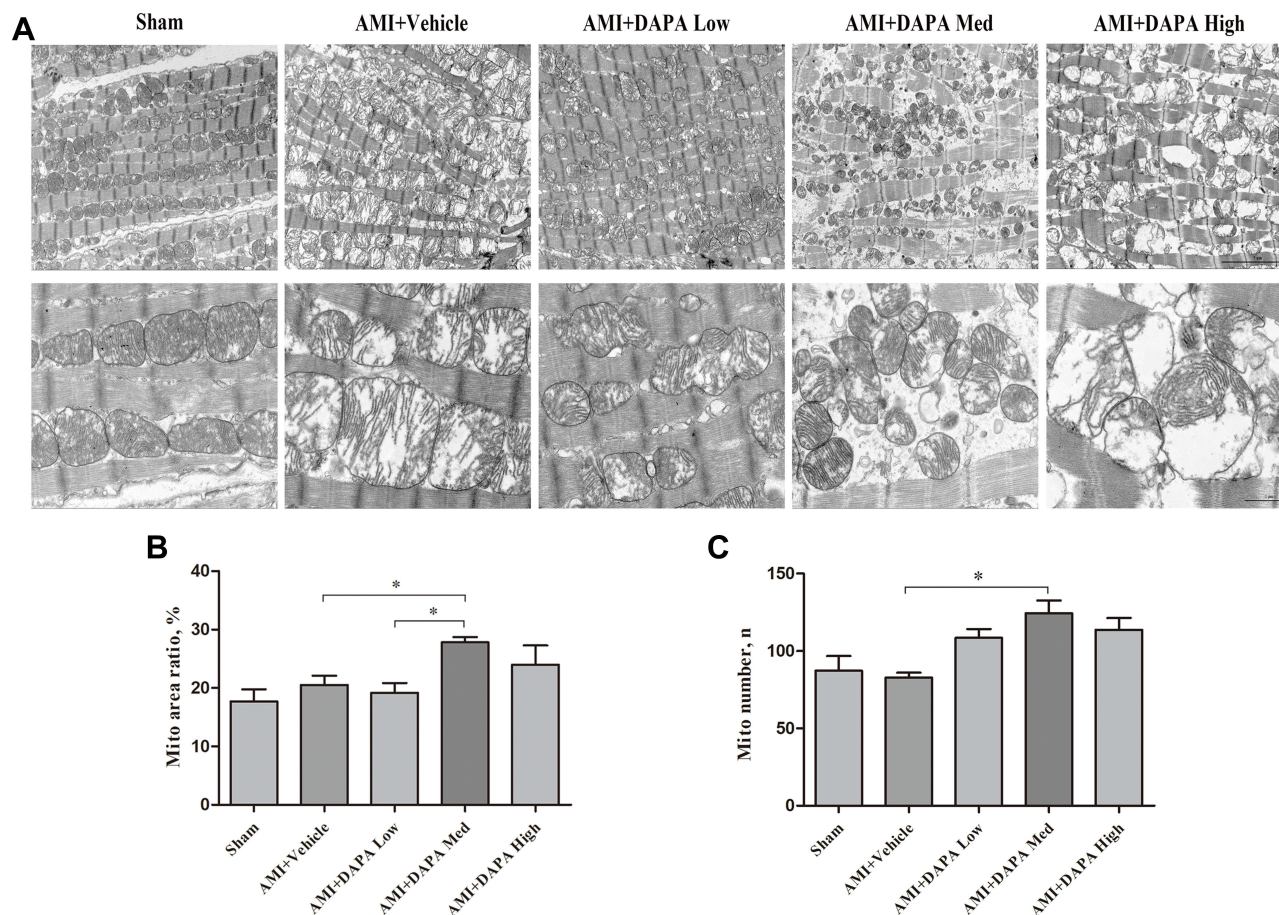


**Figure 3** Dapagliflozin normalized the mitochondrial morphology and structure among the infarcted myocardium. **(A)** Representative electron micrographs for Sham, AMI+Vehicle, AMI+DAPA Low, AMI+DAPA Med and AMI+DAPA High group, respectively. **(B)** The percentage of total mitochondrial area to the cardiomyocytes area and **(C)** mitochondrial number per area. Six images were taken from each heart, and data for 3–5 rats in each group were analyzed; Data are mean±SD. \* $P < 0.05$ .

DAPA treatment could significantly upregulate it (Figure 4D). Besides, TUNEL staining results showed fewer positive cardiac cells occurred in the DAPA groups when compared to the AMI+Vehicle group (Figure 5). Similarly, the DAPA Med group showed a better result, indicating that DAPA might also have an anti-apoptosis effect in MI and that a medium dose of DAPA treatment was more preferred.

## Experiments in vitro

H9c2 cell lines were subjected to hypoxic treatment to investigate the cardioprotective role of DAPA. Although the cell lines incubated in hypoxic condition for 48 hours appeared the highest effects on target genes (Figure 6), most of the cells in the cultural mediums died under the microscopy from visual assessment. Therefore, we decided to incubate the cell lines under hypoxic condition for 24 hours for further experiments.

### Dapagliflozin Activates PGAM5 to Upregulate the Expression of Drp1 and then Reduce Cardiomyocyte Apoptosis

Similarly, DAPA could upregulate the expression of Drp1 when subjecting to hypoxic condition, as well as the expression of PGAM5 (Figure 7A and B). The protein levels of mfn1 and mfn2 showed no significance between the Hypoxia group and Hypoxia+DAPA group (Figure 7C and D). Besides, the total caspase3 expression was significantly inhibited by DAPA treatment (Figure 7E), indicating the reduction of cell apoptosis which was in line with that from TUNEL staining results.

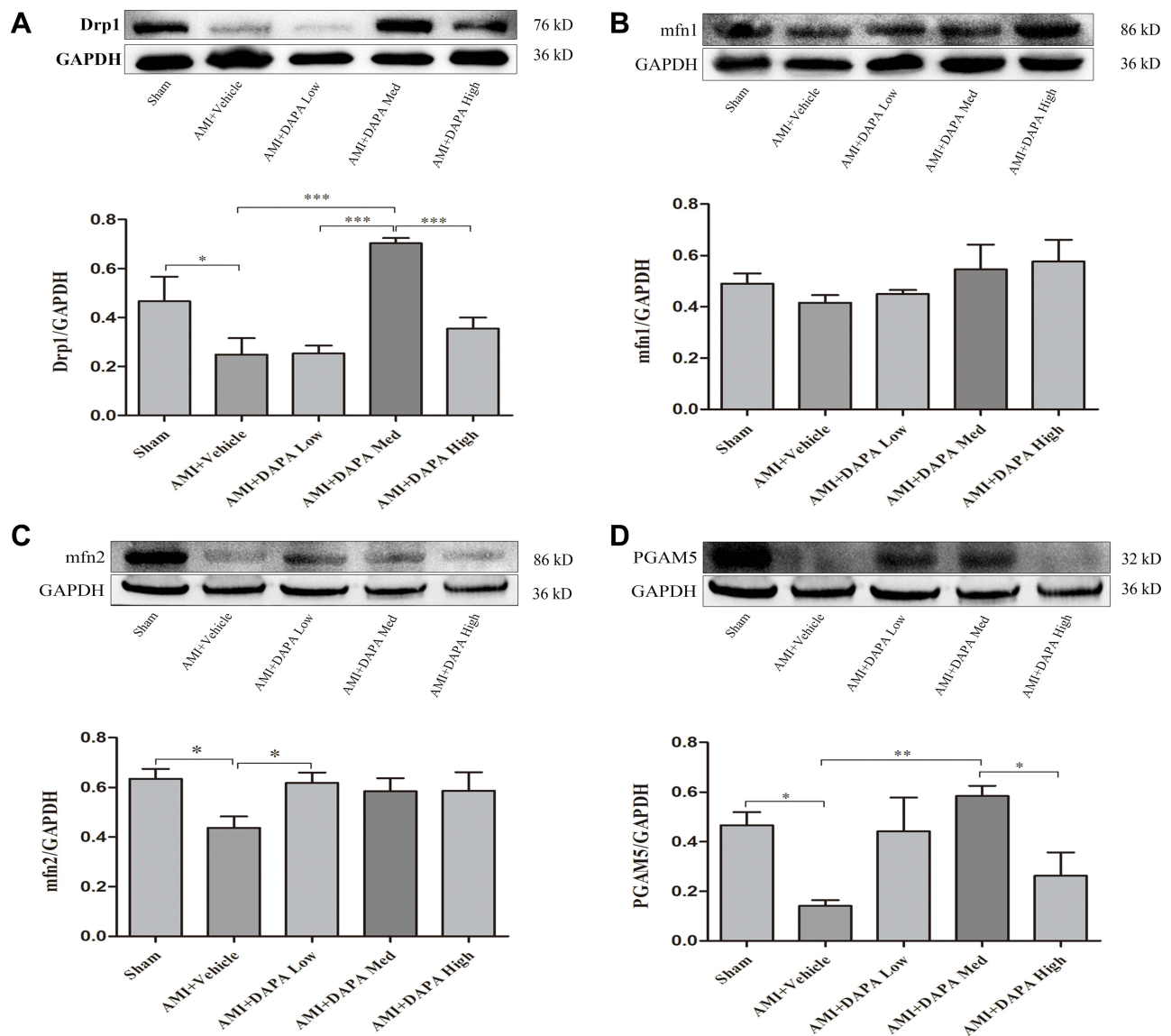


**Figure 4** Representative Western blots of heart tissues and quantitative analyses for dynamin-related protein 1 (DRP1) (A), phosphoglycerate mutase 5 (PGAM5) (B), fusion protein mitofusin 1 (Mfn1) (C), and fusion protein mitofusin 2 (Mfn2) (D) protein expression levels normalized to GAPDH.  $N \geq 3$  per; Data are mean  $\pm$  SD. \* $P < 0.05$ , \*\* $P < 0.01$ , \*\*\* $P < 0.001$ .

To confirm the mediating effects of DAPA, we suppressed the expression of PGAM5 via a specific siRNA (Figure 8A). When comparing the siRNA+DAPA group versus the siRNA group, the upregulating effect on PGAM5 induced by DAPA was completely counteracted after transfecting with siRNA (Figure 8B), as well as the upregulated expression of Drp1 (Figure 8C). Moreover, the total caspase3 expression was significantly increased after inhibiting PGAM5, and the downregulation of total caspase3 induced by DAPA treatment was also subsequently dismissed (Figure 8D). In a summary, these results showed that DAPA could induce an activation of PGAM5 to upregulate Drp1 and then played as an anti-apoptosis role.

## Discussion

In the present study, we established an AMI model for non-diabetic SD rats and applied DAPA treatment at different concentrations along an increased gradient for 6 weeks. The alleviation of cardiac remodeling post MI and improved cardiac function were strongly associated with DAPA treatment, which would not affect kidney function and serum electrolyte levels ( $K^+$ ,  $Na^+$  and P). The underlying mechanisms might be related to the activation of PGAM5-Drp1 axis,

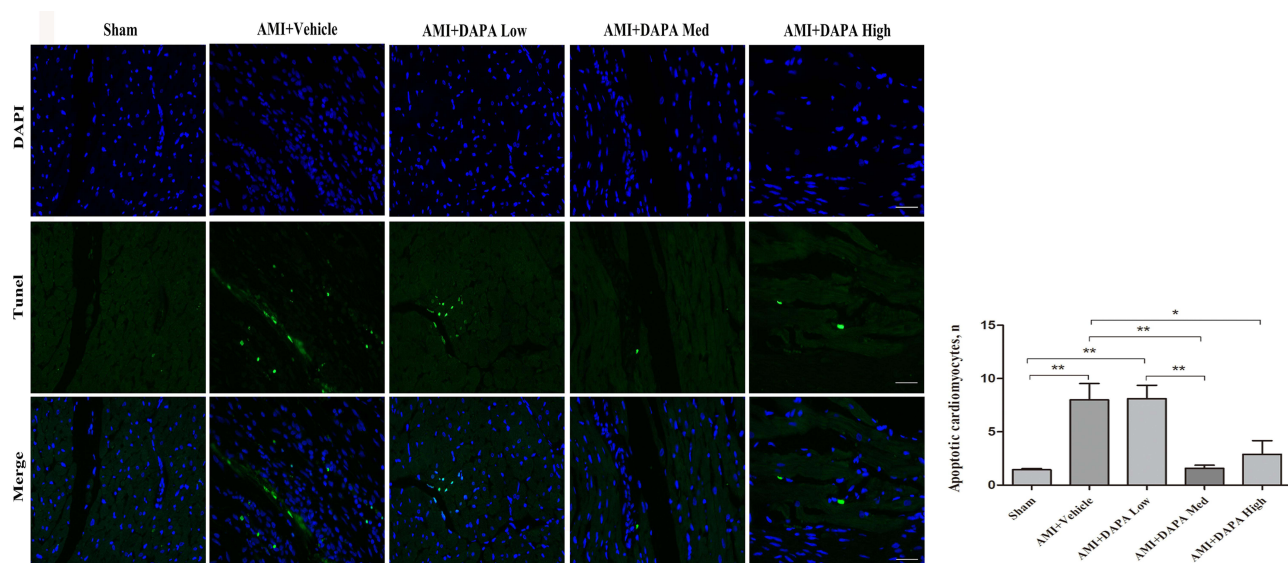


**Figure 5** Dapagliflozin attenuated myocardial apoptosis at 6 weeks after MI. (A) Representative TUNEL staining images for Sham, AMI+Vehicle, AMI+DAPA Low, AMI+DAPA Med and AMI+DAPA High group, respectively. Green: TUNEL positive cells, blue: DAPI. (B) Counts of apoptotic cells among the infarcted myocardium.  $N \geq 3$  per; Data are mean  $\pm$  SD. \* $P < 0.05$ , \*\* $P < 0.01$ .

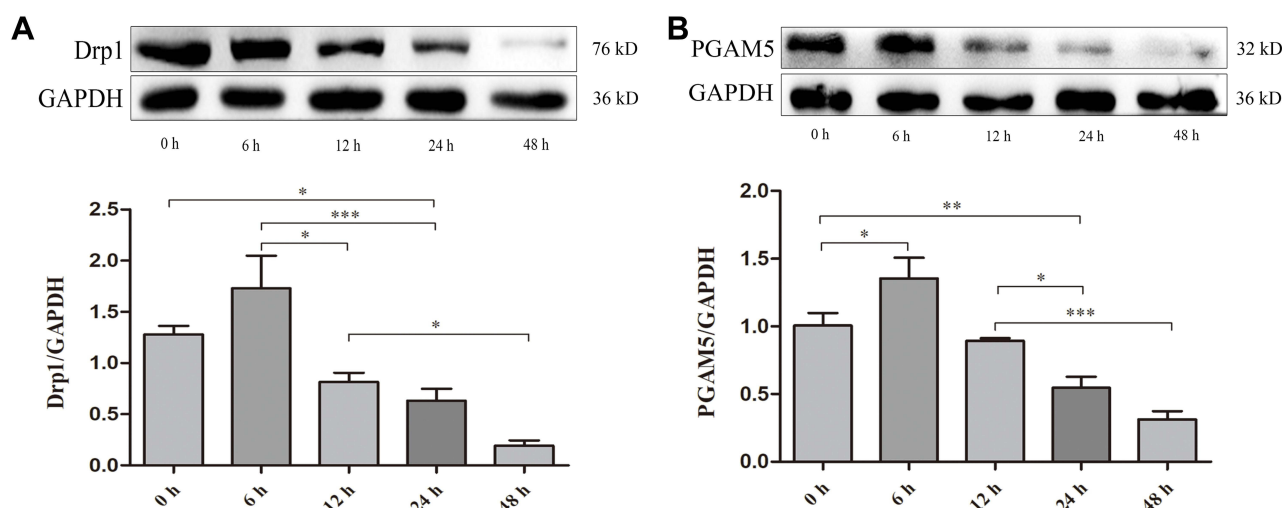


**Figure 6** Time gradient experiment identified 24h as the optimal tolerance duration of H9c2 cell lines to the hypoxic treatment. (A) Representative Western blots and quantitative analyses for Drp1 and (B) PGAM5 protein expression levels normalized to GAPDH.  $N \geq 3$  per; Data are mean  $\pm$  SD. \* $P < 0.05$ , \*\* $P < 0.01$ , \*\*\* $P < 0.001$ .

consequently normalizing the mitochondrial fission and reducing cardiomyocyte apoptosis. Moreover, an appropriate dose of DAPA treatment would work better in MI.

The inevitable cardiac remodeling post MI causes cardiac dysfunction easily, triggering HF and sudden cardiac death, leading to a high mortality rate.<sup>32,33</sup> Recently, several large and powerful RCTs indicated that SGLT2i could decrease the risk of worsening HF or cardiac death in HF patients without diabetes.<sup>13–15</sup> Accordingly, SGLT2i were strongly recommended as a routine medical therapy for HF in the latest AHA/ACC guidelines, especially for these patients with HFrEF (Ia).<sup>34</sup> Nonetheless, the dose and time for administering SGLT2i were still confused in clinical practice. A recent study published by Wang et al<sup>21</sup> revealed that DAPA could improve the cardiac function after MI via inhibiting the PI3K/AKT/mTOR pathway. However, the dose of DAPA they used was not intended for clinical practice in the real world. To explore for a widely used dose and time of DAPA for MI, as well as the potential mechanisms, we conducted this present study.

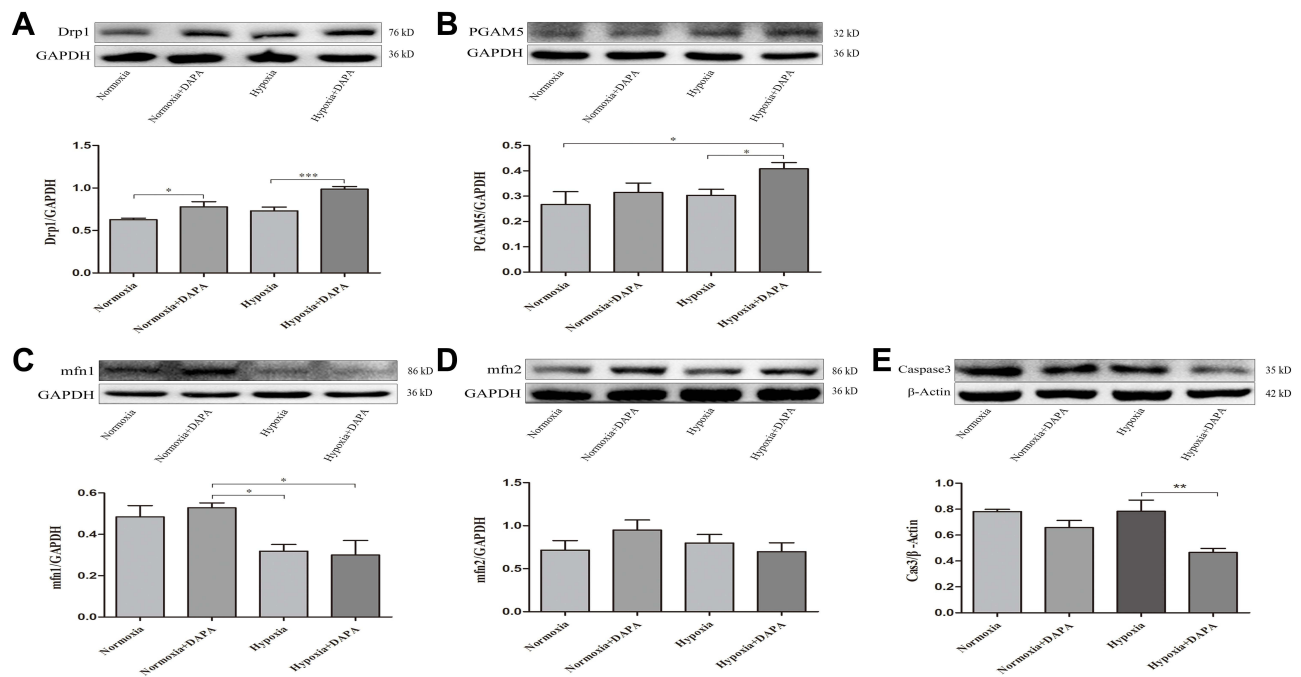


**Figure 7** Representative Western blots of H9c2 cells and quantitative analyses for Drp1 (A), PGAM5 (B), Mfn1 (C), and Mfn2 (D) protein expression levels normalized to GAPDH. (E) Quantitative analysis for total caspase3 protein expression level was normalized to  $\beta$ -Actin. N $\geq$ 3 per. \* $P < 0.05$ , \*\* $P < 0.01$ , \*\*\* $P < 0.001$ .

The commonly accepted concept responsible for these benefits of SGLT2i in HF could be derived from the fact that SGLT2i are potent proximal tubule diuretics, which could reduce the preload and afterload of heart and then decrease the myocardial oxygen demand to release the HF symptoms.<sup>11,35</sup> Simultaneously, the relatively increased hematocrit after diuresis would also enhance the supply of oxygen to myocardial cells. Besides, glucose excretion would promote lipid decomposition to increase the myocardial ketone, serving as a more effective productivity substrate to improve the production and storage of mitochondrial ATP in cardiomyocytes.<sup>36,37</sup> In our study, attenuated cardiac fibrosis and improved cardiac function were found with respect to DAPA treatment and the medium dose of DAPA seemed to be more superior. The positive results might mainly be due to the normalization of MI-induced damage to the mitochondrial morphology and structure, which would be helpful to improve the cardiac metabolism and were in line with that from several previous studies.<sup>16,17,37</sup> Moreover, Drp1 and mfn1/2 had been noted as key mediators of mitochondrial dynamism (fission and fusion) to control the mitochondrial quality.<sup>29</sup> Consistently, Western blotting analyses also indicated an upregulation of Drp1 after receiving a medium dose of DAPA treatment, while there was no significance in mfn1/mfn2 when comparing the DAPA Med group to AMI+Vehicle group. A prior study reported that conditional deletion of both Drp1 and Mfn1/Mfn2 could induce progressive LV enlargement and a decline in ejection performance.<sup>27</sup> As a result, this might also be a potential explanation for the partly improved remodeling post MI with respect to the DAPA treatment. Neither low nor high dose of DAPA treatment showed similar positive effects.

Since the apoptosis was initially described in MI, it had been kept for researching as an important therapeutic target in the pathological process.<sup>38,39</sup> Occlusion of the culprit coronary artery induced the complete loss of blood flow to the myocardium, leading to a large amount of cardiomyocyte apoptosis.<sup>3</sup> The following decreased number of myocytes and contractile units would significantly reduce the myocardial contractility.<sup>40</sup> Results from our study indicated that DAPA treatment, especially the medium dose of DAPA, could significantly reduce the cardiomyocyte apoptosis among the infarcted myocardium, contributing to better cardiac functions. Additionally, the decreased serum  $\text{Ca}^{2+}$  in AMI+Vehicle group could be compensatively increased after receiving DAPA treatment. A prior study reported that the elevation of cytoplasmic  $\text{Na}^+$  and  $\text{Ca}^{2+}$  might worsen the pathology of HF, while SGLT2i might directly inhibit the  $\text{Na}^+/\text{H}^+$  exchanger, leading to a reduction of cytoplasmic  $\text{Na}^+$  and  $\text{Ca}^{2+}$ , thus offering cardiac protective effects.<sup>41</sup> This would also be an explanation for the improved cardiac function with respect to DAPA treatment and needed for further explorations.

PGAM5 is a mitochondrial membrane protein with homology in a superfamily of phosphoglycerate mutases,<sup>31</sup> and has been reported to be involved in a giant number of important biological functions, such as mitophagy,<sup>42</sup> apoptosis,<sup>43</sup>

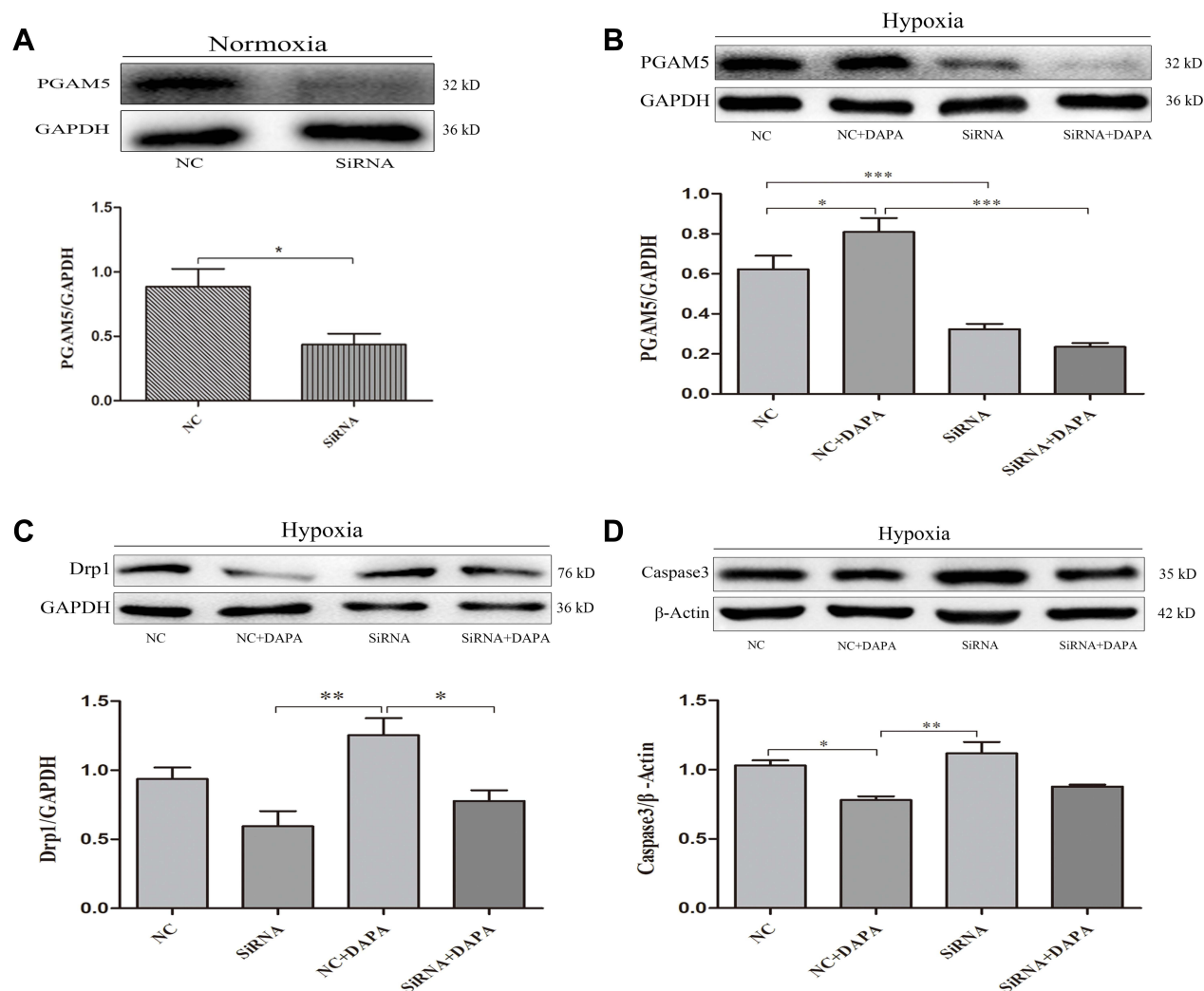


**Figure 8** Dapagliflozin activated the PGAM5/Drp1 signaling pathway in MI. **(A)** Western blot and quantitative analysis confirmed the suppression of PGAM5 with respect to the specific siRNA in H9c2 cells. **(B)** Representative Western blots and quantitative analyses for PGAM5 and **(C)** Drp1. The GAPDH was set as an internal reference. **(D)** Western blot and quantitative analysis for total caspase3 protein expression levels normalized to  $\beta$ -Actin.  $N \geq 3$  per; Data are mean  $\pm$  SD. \* $P < 0.05$ , \*\* $P < 0.01$ , \*\*\* $P < 0.001$ .

necroptosis,<sup>44</sup> and inflammation.<sup>45</sup> Yang et al<sup>46</sup> priorly revealed that PGAM5 could control cardiomyocyte apoptosis via regulating Keap1-mediated Bcl-xL degradation in ischemia/reperfusion injury. Consistently, TUNEL staining in heart tissues combined with Western blotting analyses in our study also demonstrated the protective effects of PGAM5 on cardiomyocytes from apoptosis induced by MI. Next, we suppressed the expression of PGAM5 in H9c2 cells through a specific siRNA and found that the upregulation of PGAM5 induced by DAPA would be completely counteracted under the hypoxic condition, as well as the upregulated expression of Drp1. Moreover, a significant increase in total caspase3 was found after inhibiting PGAM5, and the downregulation of total caspase3 induced by DAPA treatment was also subsequently dismissed. These in vivo and in vitro results suggested that DAPA on cardiac function, remodeling, normalization of mitochondrial fission, and cell apoptosis might be related to the activation of the PGAM5/Drp1 signaling pathway.

## Limitations

There are several limitations involved in this study that should be acknowledged. First, our study was mainly designed for assessing the myocardial effects following different treatment doses of DAPA for MI, and we did not focus on the indexes related to cardiac metabolism (ATP detection, mitochondrial DNA and nuclear DNA among infarcted myocardium, etc.) because there had been many researches demonstrating the positive results with respect to DAPA treatment.<sup>18,37</sup> Second, the sample size of SD rats was still relatively small as many cases died of heart rupture,

ventricular fibrillation or pneumothorax during or after the surgery procedures. Third, we harvested the heart tissues for further detection at 6 weeks after MI operation, which would limit us determining the relevant effects of DAPA on the early stage of MI. Fourth, the assessment of the damage to bladder endothelium with respect to DAPA was mainly relied on HE staining results, without any quantitative analyses. At last, the agonist for PGAM5/Drp1 pathway was absent in the experimental groups, which might partly limit a better understanding of the stated mechanisms.

## Conclusion

Appropriate doses of DAPA could improve cardiac remodeling and cardiac function post MI by normalizing the mitochondrial fission and reducing cardiomyocyte apoptosis, without increased damage to the bladder endothelium following higher treatment doses. The underlying mechanisms might be associated with the activation of PGAM5/Drp1 signaling pathway. Our results might provide some new insights into the benefits of DAPA treatment as an initial adjunctive regimen for AMI patients without diabetes.

## Funding

The present study was supported by the National Natural Science Foundation of China (granted number 82070295) and Jiangsu Provincial Key Medical Discipline (Laboratory ZDXKA2016023).

## Disclosures

The authors report no conflicts of interest in this work.

## References

1. Reed GW, Rossi JE, Cannon CP. Acute myocardial infarction. *Lancet*. 2017;389(10065):197–210. doi:10.1016/S0140-6736(16)30677-8
2. Benjamin EJ, Virani SS, Callaway CW, et al. Heart disease and stroke statistics-2018 update: a report from the American Heart Association. *Circulation*. 2018;137(12):e67–e492. doi:10.1161/CIR.0000000000000558
3. Virani SS, Alonso A, Benjamin EJ, et al. Heart disease and stroke statistics-2020 update: a report from the American Heart Association. *Circulation*. 2020;141(9):e139–e596. doi:10.1161/CIR.0000000000000757
4. Uygur A, Lee RT. Mechanisms of cardiac regeneration. *Dev Cell*. 2016;36(4):362–374. doi:10.1016/j.devcel.2016.01.018
5. Ezekowitz JA, O'Meara E, McDonald MA, et al. 2017 Comprehensive update of the Canadian cardiovascular society guidelines for the management of heart failure. *Can J Cardiol*. 2017;33(11):1342–1433. doi:10.1016/j.cjca.2017.08.022
6. American Diabetes A. 9. Cardiovascular disease and risk management: standards of medical care in diabetes-2018. *Diabetes Care*. 2018;41(Suppl 1):S86–S104.
7. Zhao M, Nakada Y, Wei Y, et al. Cyclin D2 overexpression enhances the efficacy of human induced pluripotent stem cell-derived cardiomyocytes for myocardial repair in a swine model of myocardial infarction. *Circulation*. 2021;144(3):210–228. doi:10.1161/CIRCULATIONAHA.120.049497
8. Devarakonda T, Mauro AG, Cain C, Das A, Salloum FN. Cardiac gene therapy with relaxin receptor 1 overexpression protects against acute myocardial infarction. *JACC Basic Transl Sci*. 2022;7(1):53–63. doi:10.1016/j.jacbts.2021.10.012
9. Neumann FJ, Sousa-Uva M, Ahlsson A, et al. 2018 ESC/EACTS Guidelines on myocardial revascularization. *Eur Heart J*. 2019;40(2):87–165. doi:10.1093/eurheartj/ehy394
10. Yang Y, Cheng HW, Qiu Y, et al. MicroRNA-34a plays a key role in cardiac repair and regeneration following myocardial infarction. *Circ Res*. 2015;117(5):450–459. doi:10.1161/CIRCRESAHA.117.305962
11. Kuhre RE, Ghiasi SM, Adriaenssens AE, et al. No direct effect of SGLT2 activity on glucagon secretion. *Diabetologia*. 2019;62(6):1011–1023. doi:10.1007/s00125-019-4849-6
12. Wiviott SD, Raz I, Bonaca MP, et al. Dapagliflozin and cardiovascular outcomes in type 2 diabetes. *N Engl J Med*. 2019;380(4):347–357. doi:10.1056/NEJMoa1812389
13. McMurray JJV, Solomon SD, Inzucchi SE, et al. Dapagliflozin in Patients with heart failure and reduced ejection fraction. *N Engl J Med*. 2019;381(21):1995–2008. doi:10.1056/NEJMoa1911303
14. Packer M, Anker SD, Butler J, et al. Cardiovascular and renal outcomes with empagliflozin in heart failure. *N Engl J Med*. 2020;383(15):1413–1424. doi:10.1056/NEJMoa2022190
15. Anker SD, Butler J, Filippatos G, et al. Empagliflozin in heart failure with a preserved ejection fraction. *N Engl J Med*. 2021;385(16):1451–1461. doi:10.1056/NEJMoa2107038
16. Tanajak P, Sa-Nguanmoo P, Sivasinprasasn S, et al. Cardioprotection of dapagliflozin and vildagliptin in rats with cardiac ischemia-reperfusion injury. *J Endocrinol*. 2018;236(2):69–84. doi:10.1530/JOE-17-0457
17. Mizuno M, Kuno A, Yano T, et al. Empagliflozin normalizes the size and number of mitochondria and prevents reduction in mitochondrial size after myocardial infarction in diabetic hearts. *Physiol Rep*. 2018;6(12):e13741. doi:10.14814/phy2.13741
18. Adingupu DD, Gopel SO, Gronros J, et al. SGLT2 inhibition with empagliflozin improves coronary microvascular function and cardiac contractility in prediabetic ob/ob(-/-) mice. *Cardiovasc Diabetol*. 2019;18(1):16. doi:10.1186/s12933-019-0820-6
19. Oshima H, Miki T, Kuno A, et al. Empagliflozin, an SGLT2 inhibitor, reduced the mortality rate after acute myocardial infarction with modification of cardiac metabolomes and antioxidants in diabetic rats. *J Pharmacol Exp Ther*. 2019;368(3):524–534. doi:10.1124/jpet.118.253666

20. Lee TM, Chang NC, Lin SZ. Dapagliflozin, a selective SGLT2 inhibitor, attenuated cardiac fibrosis by regulating the macrophage polarization via STAT3 signaling in infarcted rat hearts. *Free Radic Biol Med.* 2017;104:298–310. doi:10.1016/j.freeradbiomed.2017.01.035
21. Wang K, Li Z, Sun Y, et al. Dapagliflozin improves cardiac function, remodeling, myocardial apoptosis, and inflammatory cytokines in mice with myocardial infarction. *J Cardiovasc Transl Res.* 2021. doi:10.1007/s12265-021-10192-y
22. Liu Y, Wu M, Xu J, Xu B, Kang L. Empagliflozin prevents from early cardiac injury post myocardial infarction in non-diabetic mice. *Eur J Pharm Sci.* 2021;161:105788. doi:10.1016/j.ejps.2021.105788
23. Percie du Sert N, Hurst V, Ahluwalia A, et al. The ARRIVE guidelines 2.0: updated guidelines for reporting animal research. *BMC Vet Res.* 2020;16(1):242. doi:10.1186/s12917-020-02451-y
24. van der Meer P, Lipsic E, Henning RH, et al. Erythropoietin induces neovascularization and improves cardiac function in rats with heart failure after myocardial infarction. *J Am Coll Cardiol.* 2005;46(1):125–133. doi:10.1016/j.jacc.2005.03.044
25. Fan ZG, Qu XL, Chu P, et al. MicroRNA-210 promotes angiogenesis in acute myocardial infarction. *Mol Med Rep.* 2018;17(4):5658–5665. doi:10.3892/mmr.2018.8620
26. Shao Q, Meng L, Lee S, et al. Empagliflozin, a sodium glucose co-transporter-2 inhibitor, alleviates atrial remodeling and improves mitochondrial function in high-fat diet/streptozotocin-induced diabetic rats. *Cardiovasc Diabetol.* 2019;18(1):165. doi:10.1186/s12933-019-0964-4
27. Song M, Mihara K, Chen Y, Scorrano L, Dorn GW. Mitochondrial fission and fusion factors reciprocally orchestrate mitophagic culling in mouse hearts and cultured fibroblasts. *Cell Metab.* 2015;21(2):273–286. doi:10.1016/j.cmet.2014.12.011
28. Kapur NK, Heffernan KS, Yunis AA, et al. Usefulness of soluble endoglin as a noninvasive measure of left ventricular filling pressure in heart failure. *Am J Cardiol.* 2010;106(12):1770–1776. doi:10.1016/j.amjcard.2010.08.018
29. Twig G, Elorza A, Molina AJ, et al. Fission and selective fusion govern mitochondrial segregation and elimination by autophagy. *EMBO J.* 2008;27(2):433–446. doi:10.1038/sj.emboj.7601963
30. Aravind L, Dixit VM, Koonin EV. Apoptotic molecular machinery: vastly increased complexity in vertebrates revealed by genome comparisons. *Science.* 2001;291(5507):1279–1284. doi:10.1126/science.291.5507.1279
31. Lu W, Sun J, Yoon JS, et al. Mitochondrial Protein PGAM5 regulates mitophagic protection against cell necroptosis. *PLoS One.* 2016;11(1):e0147792. doi:10.1371/journal.pone.0147792
32. Matboli M, Shafei AE, Agwa SHA, et al. Identification of novel molecular network expression in acute myocardial infarction. *Curr Genomics.* 2019;20(5):340–348. doi:10.2174/1389202920666190820142043
33. Brooks GC, Lee BK, Rao R, et al. Predicting persistent left ventricular dysfunction following myocardial infarction: the PREDICTS study. *J Am Coll Cardiol.* 2016;67(10):1186–1196. doi:10.1016/j.jacc.2015.12.042
34. Heidenreich PA, Bozkurt B, Aguilar D, et al. 2022 AHA/ACC/HFSA guideline for the management of heart failure: a report of the American College of Cardiology/American Heart Association joint committee on clinical practice guidelines. *Circulation.* 2022;79:e263–421.
35. de Leeuw AE, de Boer RA. Sodium-glucose cotransporter 2 inhibition: cardioprotection by treating diabetes—a translational viewpoint explaining its potential salutary effects. *Eur Heart J Cardiovasc Pharmacother.* 2016;2(4):244–255. doi:10.1093/ehjcvp/pvw009
36. Ferrannini E, Mark M, Mayoux E. CV Protection in the EMPA-REG OUTCOME trial: a “Thrifty Substrate” hypothesis. *Diabetes Care.* 2016;39(7):1108–1114. doi:10.2337/dc16-0330
37. Yurista SR, Sillje HHW, Oberdorf-Maass SU, et al. Sodium-glucose co-transporter 2 inhibition with empagliflozin improves cardiac function in non-diabetic rats with left ventricular dysfunction after myocardial infarction. *Eur J Heart Fail.* 2019;21(7):862–873. doi:10.1002/ejhf.1473
38. Gottlieb RA, Burleson KO, Kloner RA, Babior BM, Engler RL. Reperfusion injury induces apoptosis in rabbit cardiomyocytes. *J Clin Invest.* 1994;94(4):1621–1628. doi:10.1172/JCI117504
39. Takemura G, Fujiwara H. Role of apoptosis in remodeling after myocardial infarction. *Pharmacol Ther.* 2004;104(1):1–16. doi:10.1016/j.pharmthera.2004.07.005
40. Jose Corbalan J, Vatner DE, Vatner SF. Myocardial apoptosis in heart disease: does the emperor have clothes? *Basic Res Cardiol.* 2016;111(3):31. doi:10.1007/s00395-016-0549-2
41. Verma S, McMurray JJV. SGLT2 inhibitors and mechanisms of cardiovascular benefit: a state-of-the-art review. *Diabetologia.* 2018;61(10):2108–2117. doi:10.1007/s00125-018-4670-7
42. Chen G, Han Z, Feng D, et al. A regulatory signaling loop comprising the PGAM5 phosphatase and CK2 controls receptor-mediated mitophagy. *Mol Cell.* 2014;54(3):362–377. doi:10.1016/j.molcel.2014.02.034
43. Ishida Y, Sekine Y, Oguchi H, et al. Prevention of apoptosis by mitochondrial phosphatase PGAM5 in the mushroom body is crucial for heat shock resistance in *Drosophila melanogaster*. *PLoS One.* 2012;7(2):e30265. doi:10.1371/journal.pone.0030265
44. Murphy JM, Czabotar PE, Hildebrand JM, et al. The pseudokinase MLKL mediates necroptosis via a molecular switch mechanism. *Immunity.* 2013;39(3):443–453. doi:10.1016/j.immuni.2013.06.018
45. Kang YJ, Bang BR, Han KH, et al. Regulation of NKT cell-mediated immune responses to tumours and liver inflammation by mitochondrial PGAM5-Drp1 signalling. *Nat Commun.* 2015;6:8371. doi:10.1038/ncomms9371
46. Yang C, Liu X, Yang F, et al. Mitochondrial phosphatase PGAM5 regulates Keap1-mediated Bcl-xL degradation and controls cardiomyocyte apoptosis driven by myocardial ischemia/reperfusion injury. *In Vitro Cell Dev Biol Anim.* 2017;53(3):248–257. doi:10.1007/s11626-016-0105-2

## Drug Design, Development and Therapy

Dovepress

### Publish your work in this journal

Drug Design, Development and Therapy is an international, peer-reviewed open-access journal that spans the spectrum of drug design and development through to clinical applications. Clinical outcomes, patient safety, and programs for the development and effective, safe, and sustained use of medicines are a feature of the journal, which has also been accepted for indexing on PubMed Central. The manuscript management system is completely online and includes a very quick and fair peer-review system, which is all easy to use. Visit <http://www.dovepress.com/testimonials.php> to read real quotes from published authors.

Submit your manuscript here: <https://www.dovepress.com/drug-design-development-and-therapy-journal>